
This is an electronic reprint of the original article.
This reprint *may differ* from the original in pagination and typographic detail.

Author(s): Li, H. J.; Cederwall, B.; Bäck, T.; Qi, C.; Doncel, M.; Jakobsson, Ulrika; Auranen, Kalle; Bönig, S.; Drummond, M. C.; Grahn, Tuomas; Greenlees, Paul; Herzan, Andrej; Julin, Rauno; Juutinen, Sakari; Konki, Joonas; Kröll, T.; Leino, Matti; McPeake, C.; O'Donnell, D.; Page, R. D.; Pakarinen, Janne; Partanen, Jari; Peura, Pauli; Rahkila, Panu; Ruotsalainen, Panu; Sandzelius, Mikael; Sarén, Jan; Saygi, B.; Scholey, Catherine; Sorri, Jukka; Stolz, Stefan; Taylor, M. J.; Thorsen, A.; Uusitalo, Jukka; Xiao, Z. G.

Title: Recoil-decay tagging spectroscopy of ^{162}W 88

Year: 2015

Version:

Please cite the original version:

Li, H. J., Cederwall, B., Bäck, T., Qi, C., Doncel, M., Jakobsson, U., Auranen, K., Bönig, S., Drummond, M. C., Grahn, T., Greenlees, P., Herzan, A., Julin, R., Juutinen, S., Konki, J., Kröll, T., Leino, M., McPeake, C., O'Donnell, D., . . . Xiao, Z. G. (2015). Recoil-decay tagging spectroscopy of ^{162}W 88. *Physical Review C*, 92(1), Article 014326. <https://doi.org/10.1103/PhysRevC.92.014326>

All material supplied via JYX is protected by copyright and other intellectual property rights, and duplication or sale of all or part of any of the repository collections is not permitted, except that material may be duplicated by you for your research use or educational purposes in electronic or print form. You must obtain permission for any other use. Electronic or print copies may not be offered, whether for sale or otherwise to anyone who is not an authorised user.

Recoil-decay tagging spectroscopy of $^{162}_{74}\text{W}_{88}$

H. J. Li,^{1,2,*} B. Cederwall,¹ T. Bäck,¹ C. Qi,¹ M. Doncel,¹ U. Jakobsson,^{1,3} K. Auranen,³ S. Bönig,⁴ M. C. Drummond,⁵ T. Grahn,³ P. Greenlees,³ A. Herzán,³ R. Julin,³ S. Juutinen,³ J. Konki,³ T. Kröll,⁴ M. Leino,³ C. McPeake,⁵ D. O'Donnell,⁵ R. D. Page,⁵ J. Pakarinen,³ J. Partanen,³ P. Peura,^{3,†} P. Rähkila,³ P. Ruotsalainen,^{3,‡} M. Sandzelius,³ J. Sarén,³ B. Saygi,^{5,§} C. Scholey,³ J. Sorri,³ S. Stolze,³ M. J. Taylor,⁶ A. Thornthwaite,⁵ J. Uusitalo,³ and Z. G. Xiao²

¹Department of Physics, KTH-Royal Institute of Technology, SE-10691 Stockholm, Sweden

²Department of Physics, Tsinghua University, Beijing 100084, People's Republic of China

³University of Jyväskylä, Department of Physics, P.O. Box 35, FI-40014 University of Jyväskylä, Finland

⁴Institut für Kernphysik, TU Darmstadt, D-64289 Darmstadt, Germany

⁵Department of Physics, Oliver Lodge Laboratory, University of Liverpool, Liverpool L69 7ZE, United Kingdom

⁶School of Physics and Astronomy, University of Manchester, Manchester M13 9PL, United Kingdom

(Received 27 May 2015; published 30 July 2015)

Excited states in the highly neutron-deficient nucleus ^{162}W have been investigated via the $^{92}\text{Mo}(^{78}\text{Kr}, 2\alpha)^{162}\text{W}$ reaction. Prompt γ rays were detected by the JUROGAM II high-purity germanium detector array and the recoiling fusion-evaporation products were separated by the recoil ion transport unit (RITU) gas-filled recoil separator and identified with the gamma recoil electron alpha tagging (GREAT) spectrometer at the focal plane of RITU. γ rays from ^{162}W were identified uniquely using mother-daughter and mother-daughter-granddaughter α -decay correlations. The observation of a rotational-like ground-state band is interpreted within the framework of total Routhian surface (TRS) calculations, which suggest an axially symmetric ground-state shape with a γ -soft minimum at $\beta_2 \approx 0.15$. Quasiparticle alignment effects are discussed based on cranked shell model calculations. New measurements of the ^{162}W ground-state α -decay energy and half-life were also performed. The observed α -decay energy agrees with previous measurements. The half-life of ^{162}W was determined to be $t_{1/2} = 990(30)$ ms. This value deviates significantly from the currently adopted value of $t_{1/2} = 1360(70)$ ms. In addition, the α -decay energy and half-life of ^{166}Os were measured and found to agree with the adopted values.

DOI: [10.1103/PhysRevC.92.014326](https://doi.org/10.1103/PhysRevC.92.014326)

PACS number(s): 21.10.Re, 23.20.Lv, 25.70.Jj, 27.70.+q

I. INTRODUCTION

The evolution of nuclear structure in the $A \approx 160$ – 170 region of the nuclide chart is found to change significantly as a function of isospin (neutron-proton ratio). When moving away from the highly deformed regimes near the proton and neutron midshells ($Z = 66$ and $N = 104$, respectively), coexisting prolate and triaxial-oblate shapes emerge, giving rise to structures which may be associated with γ -soft rotors and weakly deformed vibrational nuclei as the spherical $Z = N = 82$ shell closures are approached (see, e.g., Refs. [1,2] and references therein). Nuclei with proton numbers $Z \approx 70$ have revealed several interesting phenomena originating from the delicate interplay between different single-particle orbitals near the Fermi surface as well as with the deformation-soft mean field. The relative proximity to the $Z = N = 82$ closed shells makes these nuclei interesting objects from the point view of the development of collective excitations from a limited number of valence quasiparticles.

In the light ($N < 90$) spherical or weakly deformed tungsten isotopes, the low-spin yrast states are expected to

be based on configurations formed by coupling the spins of a few aligned valence nucleons in the proton $h_{11/2}$ and neutron $f_{7/2}/h_{9/2}$ subshells. The valence space maximum around the nucleus ^{170}Dy is situated relatively close to the β -stability line on the neutron-rich side. The highly neutron-deficient nuclide ^{162}W is located 18 neutrons away from the lightest stable tungsten isotope. When moving so far away from stability, nuclear structure studies using conventional techniques become increasingly difficult due to steeply decreasing production cross sections and a strong competition from multiple reaction channels including prompt fission.

In the present work, excited states in ^{162}W have been identified using the recoil-decay tagging (RDT) method [3–5], exploiting the characteristic α -particle radioactivity to tag prompt γ rays detected using a highly efficient array of escape-suppressed high-purity germanium detectors. The data analysis revealed a rotational-like ground-state band structure, confirming the results reported by Dracoulis *et al.* [6].

II. EXPERIMENTAL DETAILS AND DATA ANALYSIS

Excited states in ^{162}W were populated by means of the $^{92}\text{Mo}(^{78}\text{Kr}, 2\alpha)^{162}\text{W}$ fusion-evaporation reaction at a bombarding energy of 380 MeV (note here 2α also represents the $\alpha 2p 2n$ channel). The experiment was performed at the Accelerator Laboratory of the University of Jyväskylä, Finland. A 0.6-mg/cm²-thick ^{92}Mo target was bombarded by the ^{78}Kr beam provided by the K-130 cyclotron. Lifetime measurements of excited states were performed using the

*hongjiel@kth.se

[†]Present address: University of Helsinki and Helsinki Institute of Physics, Post Office Box 64, FI-00014 Helsinki, Finland.

[‡]Present address: TRIUMF, 4004 Wesbrook Mall, Vancouver, British Columbia, Canada V6T 2A3.

[§]Present address: Department of Physics, Faculty of Science, Ege University, 35100 Bornova, Izmir, Turkey.

differential plunger for unbound nuclear states (DPUNS) device [7]. A 1.0-mg/cm² Mg degrader foil was applied to slow the recoils from $v/c = 0.044$ to $v/c = 0.034$ and was placed at nine different distances from 5 to 8000 μm downstream the target position during the irradiation. Prompt γ rays were detected by the JUROGAM II γ -detector array. Fifteen EUROGAM phase I [8] and GASP-type [9] germanium detectors were placed in two rings with five detectors at 157.6° and ten detectors at 133.6° relative to the beam direction. Twenty-four EUROBALL clover detectors [10] were placed in two rings with twelve at 104.5° and the other twelve at 75.5° relative to the beam direction. The total photo-peak efficiency was 6.0% at 1.3 MeV [11]. The separation of recoiling fusion-evaporation products from beam particles and fission products was performed by the gas-filled recoil ion transport unit (RITU) [12,13] separator. The reaction products were subsequently implanted at the focal plane of RITU into two double-sided silicon strip detectors (DSSSDs) of the gamma recoil electron alpha tagging (GREAT) [14] decay spectrometer. This composite detector installation additionally consisted of a multiwire proportional counter (MWPC), an array of Si PIN diode detectors, a planar germanium detector, and three clover-type germanium detectors. The recoiling fusion residues were discriminated from scattered beam components by means of the energy loss (ΔE) in the MWPC and the time of flight between the MWPC and the DSSSDs. A triggerless total data readout (TDR) acquisition system [15] with 10-ns time-stamp precision was used for collecting data. This allowed accurate temporal correlations to be recorded between prompt γ rays detected at the target position, recoil implants at the RITU focal plane, and their subsequent radioactive decays. For practical reasons a maximum time window of 20 s was used for studies of correlations between implantation of fusion-evaporation residues and subsequent decays in the DSSSDs.

The events were reconstructed off line using the GRAIN software package [16]. In the off-line analysis, only events that could be associated with a recoil implantation signal in the DSSSDs were selected. Prompt γ - γ coincidences were selected from the γ rays detected in JUROGAM II at a preceding time corresponding to the flight time of fusion-evaporation residues through RITU to the DSSSDs. In addition, a narrow gate on the γ - γ time difference of 140 ns was applied. Then, the events were sorted into one- and two-dimensional γ -ray energy histograms with different conditions on the subsequent signals detected in the decay spectrometer. In the off-line analysis, the RADWARE software package [17] was used to construct the level scheme.

The α -decay properties of ¹⁶²W were investigated using events where ¹⁶²W was produced as a primary reaction product as well as with events where ¹⁶²W was produced as a decay product of ¹⁶⁶Os (from the $2p2n$ -fusion-evaporation channel). Figure 1(a) shows the ¹⁶²W α -decay spectrum correlated with a recoil–mother (¹⁶⁶Os)–granddaughter (¹⁵⁸Hf) chain in the same pixel of the DSSSD implantation detectors, and gives an indication of the purity of the event selection considering random correlations. The α -decay spectrum for ¹⁶²W is produced without any time condition on its α decay but requiring about three half-lives of search time as well as energy

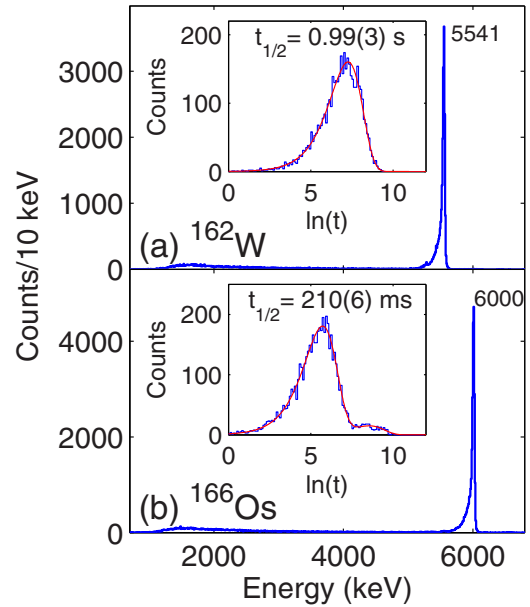


FIG. 1. (Color online) (a) Spectrum of the recorded α -decay energies from ¹⁶²W ground-state decays produced by requiring a preceding α decay from the mother nucleus ¹⁶⁶Os and a subsequent α decay from the granddaughter nucleus ¹⁵⁸Hf in the same pixel in the DSSSDs. In order to minimize the influence from random correlations, decay chains were selected for analysis by applying maximum correlation times between successive events. The maximum correlation times between recoil implantation and ¹⁶⁶Os α decay, and between ¹⁶²W α decay and ¹⁵⁸Hf α decay, were set to 0.6 and 9 s, respectively. The inset shows the distribution of time differences between mother nucleus ¹⁶⁶Os α decay and the daughter ¹⁶²W α decay. A 990(30)-ms half-life is extracted for ¹⁶²W as described in the text. (b) Spectrum showing the recorded α -decay energies of ¹⁶⁶Os produced by requiring an additional α decay from the daughter nucleus ¹⁶²W and the α decay from the granddaughter nucleus ¹⁵⁸Hf in the same pixel in the DSSSDs. The maximum correlation times between ¹⁶⁶Os α decay and ¹⁶²W α decay, and between ¹⁶²W α decay and ¹⁵⁸Hf α decay, were set to 6 and 9 s, respectively. The inset shows the distribution of time differences between implanted recoils and ¹⁶⁶Os α decays. A 210(6)-ms half-life is extracted for the ground state of ¹⁶⁶Os.

conditions on the ¹⁶⁶Os mother α decay ($t_{1/2} = 220(7)$ ms, $E_{\alpha} = 6000(6)$ keV) and ¹⁵⁸Hf granddaughter α decay ($t_{1/2} = 2850(70)$ ms, $E_{\alpha} = 5269(4)$ keV) as reported in Ref. [18]. In the spectrum, there is only evidence of the ¹⁶²W α decay with the characteristic distribution from escaped events, i.e., α particles which have left the DSSSDs without depositing their full energy. The half-life of ¹⁶²W was here determined to be $t_{1/2} = 990(30)$ ms; see the inset of Fig. 1(a). This value deviates significantly from the currently adopted value of $t_{1/2} = 1360(70)$ ms [19]. The α -decay energy for ¹⁶²W, see Fig. 1(a), is consistent with the value of $E_{\alpha} = 5541(5)$ keV measured by Page *et al.* [18]. By analyzing the distribution of time differences between implanted recoils and subsequent ¹⁶²W α decays (i.e., for events when ¹⁶²W is produced directly as a fusion product), a half-life value for ¹⁶²W consistent with the result shown in the inset of Fig. 1(a) was also obtained.

The same method was also used for measuring the half-life of ^{166}Os , as shown in Fig. 1(b). The obtained value for ^{166}Os is $t_{1/2} = 210(6)$ ms, which is consistent with the value reported by Page *et al.* [18]. This possible influence from random correlations on the determination of the half-life values was studied by analyzing subsets of the data with different pixel recoil rates. The results are found to be free from any such bias. This was also checked by means of Monte-Carlo simulations. It should also be noted that there is no bias on the measured half-lives introduced from the overall time window of 20 s applied in the analysis of recoil implants and their subsequent decays in the DSSSDs. For both the ^{166}Os and ^{162}W half-life measurements the applied maximum correlation times for the associated events in the decay chains imply that at least ten half-lives are considered in each case.

A prompt γ -ray energy spectrum recorded by JUROGAM II at the target position in delayed coincidence with a recoil detected in the DSSSDs is shown in Fig. 2(a). It is dominated by much stronger fusion-evaporation channels than the 2α -evaporation channel leading to ^{162}W ; mainly the $3pn$, $4p$, and $4pn$ channels leading to ^{166}Re , ^{166}W , and ^{165}W , respectively. The selective power of the RDT technique is illustrated in Fig. 2(b), where a recoil- α tagged prompt γ -ray spectrum is shown, obtained by selecting both the mother nucleus of ^{162}W α decays and ^{158}Hf daughter α decays with the search times between subsequent events in a given pixel of the DSSSDs set to 3 and 6 s, respectively. In this spectrum, all γ -ray lines which are indicated by their energy (in keV) are firmly assigned to originate from

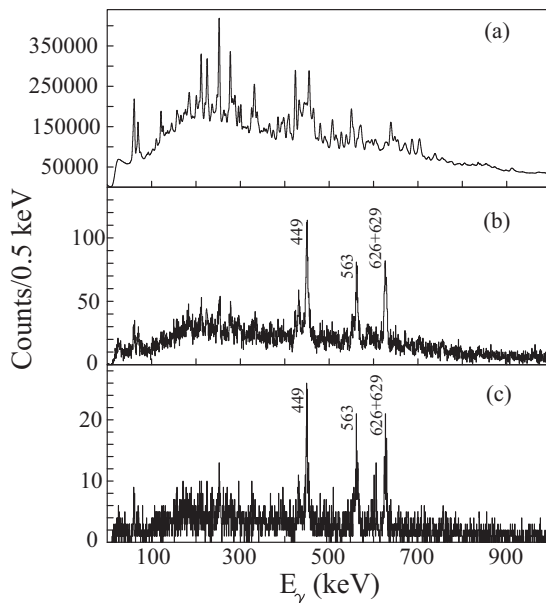


FIG. 2. (a) γ -ray spectrum of recoil-tagged singles. (b) ^{162}W mother-daughter correlated α -decay-tagged γ -ray singles. The maximum correlation time between recoils and mother nucleus (^{162}W) α decays and subsequent daughter nucleus (^{158}Hf) α decays are 3 and 6 s, respectively. The unmarked peaks are the γ -ray transitions from the strong populated channels. (c) As in panel (b) with the additional requirement of granddaughter ^{154}Yb α decay correlated within 1.2 s in the same pixel of the DSSSDs.

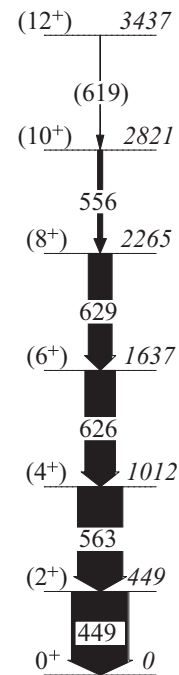


FIG. 3. Proposed level scheme for ^{162}W . Energies are given in keV. Spin and parity assignments are tentative. The widths of the arrows indicate the relative transition intensities.

decays of excited states in ^{162}W . Following implantation of ^{162}W fusion products in the DSSSDs, it was possible to follow the subsequent α -decay chain down to its end point in ^{150}Er . Both the α -decay daughter (^{158}Hf) and granddaughter (^{154}Yb) are α emitters with significant α -branching ratios of 45(3)% and 92(2)%, respectively [18]. Therefore, recoil- α - α - α correlations were also investigated. Figure 2(c) shows the recoil-mother-daughter-granddaughter correlated prompt γ -ray spectrum. This γ -ray spectrum confirms the assignment of γ rays to ^{162}W from the recoil- α - α correlated spectrum. Hence, despite the limited statistics, the clean α -correlation chain and the unique identification of γ rays with the RDT method enable a firm assignment of the identified γ rays to ^{162}W . This confirms the results reported by Dracoulis *et al.*, for which the assignment of γ -ray transitions to a specific Z value was based on coincidences with characteristic x rays [6].

The proposed level scheme deduced in this work is shown in Fig. 3. Based on the coincidence relationships and relative intensities, the γ rays assigned to ^{162}W are arranged as a cascade of stretched $E2$ transitions. The most intense 449-keV peak is hence assigned as the $(2^+) \rightarrow 0^+$ transition in ^{162}W . This agrees with the earlier report, where a plot of a γ -ray energy spectrum in coincidence with the $(2^+) \rightarrow 0^+$ 449 keV transition was shown [6].

Examples of recoil- α tagged γ -ray energy spectra for ^{162}W are shown in Fig. 4, which are obtained only from the clover detectors near 90° in order to avoid Doppler effects from the Plunger setup. Figure 4(a) presents the γ -ray spectrum coincident with the 449-keV γ -ray transition tagged by the ^{162}W α -decay energy. In this spectrum, all the γ -ray transitions above the (2^+) state in Fig. 3 are marked. The γ -ray peak

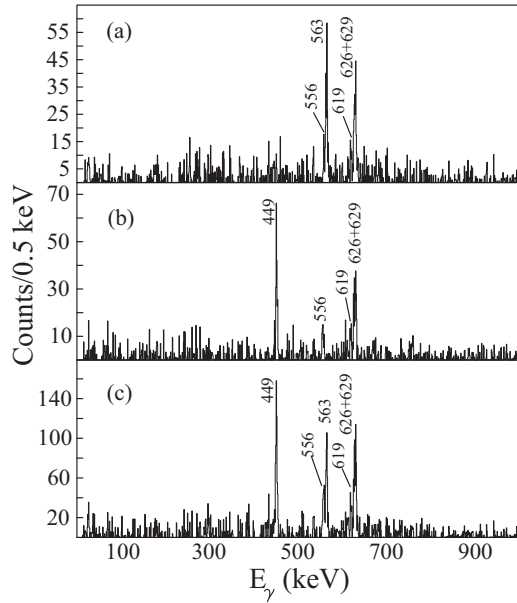


FIG. 4. Background-subtracted spectra of γ rays tagged by the ground-state α decay of ^{162}W and detected in prompt coincidence with the (a) 449-keV γ ray, (b) 563-keV γ ray, and (c) 449-, 563-, 626-, or 629-keV γ rays.

around 627 keV is regarded as a doublet based on the peak width and its self-coincident nature. The spectrum gated on the 563-keV γ -ray transition with tagging on the ^{162}W α decay is shown in Fig. 4(b). To highlight the weaker transitions in Fig. 3, a spectrum produced by adding all the gates below (8^+) is shown in Fig. 4(c). In this figure, the 556- and 629-keV γ -ray transitions can be seen more clearly. The energies, relative intensities, suggested multipolarities, and tentative spin-parity assignments of initial and final states for the γ -ray transitions assigned to ^{162}W are listed in Table I.

III. DISCUSSION

Figure 5 shows a systematic comparison between low-lying yrast excited-state level energies in neutron-deficient even- N tungsten isotopes, ranging from $N = 94$ to the lightest $N = 84$ tungsten isotope (^{158}W) for which excited states are

TABLE I. γ -ray energies, relative intensities, tentative multipolarities, and spin-parity assignments for ^{162}W . Intensities (I_γ) are adjusted for detector efficiencies and normalized to the strongest transition at $E_\gamma = 449$ keV. Statistical uncertainties are given in parentheses. Spin and parity assignments are tentative. Tentative assignments are given within parentheses.

Energy	Relative intensity	$I_i^\pi \Rightarrow I_f^\pi$	Multipolarity
449.4(3)	100	$(2^+) \Rightarrow 0^+$	($E2$)
563.1(3)	80(14)	$(4^+) \Rightarrow (2^+)$	($E2$)
556.2(6)	9(4)	$(10^+) \Rightarrow (8^+)$	($E2$)
619(1)	<1	$(12^+) \Rightarrow (10^+)$	($E2$)
625.7(3)	54(9)	$(6^+) \Rightarrow (4^+)$	($E2$)
628.6(3)	42(7)	$(8^+) \Rightarrow (6^+)$	($E2$)

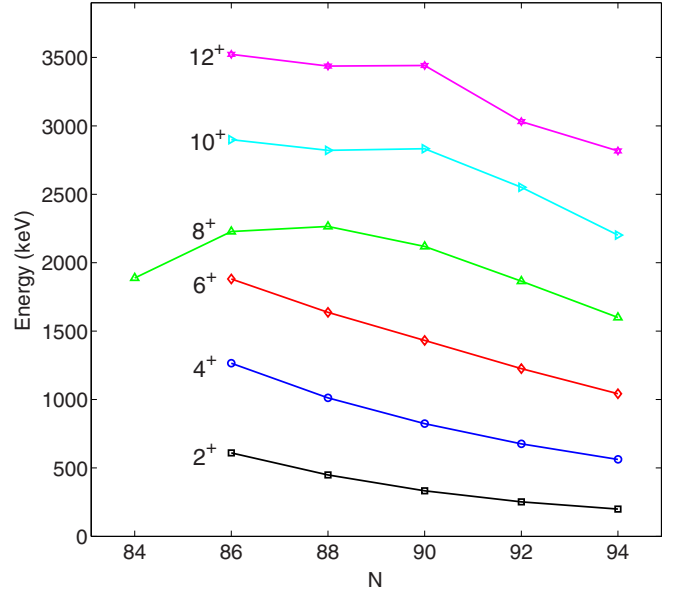


FIG. 5. (Color online) Yrast level energies in the most neutron-deficient even- N tungsten isotopes with $N = 84$ – 94 [20–24].

known. Note that the only excited state reported in ^{158}W is an α -decaying isomer at 1.888 MeV, assigned to the $\nu(f_{7/2}h_{9/2})8^+$ shell model configuration [20]. The variation of excited 8^+ state energies in ^{162}Os and neighboring nuclei has been discussed, e.g., in Ref. [25]. A gradual transition in the so-called collective character of the ground-state bands is observed, from a clear rotational-like pattern in ^{168}W to a level sequence reminiscent of near-harmonic vibrational excitations in ^{160}W . In the latter case a depression in the 8^+ level energy might be associated with the $\nu(h_{9/2})^2$ fully aligned spherical state and an onset of seniority coupling expected as the closed $N = 82$ shell is approached. The neutron number $N = 88$ appears as a transition point between the collective and spherical regimes for the tungsten isotopes.

Pairing self-consistent Woods-Saxon-Strutinsky calculations using the total Routhian surface (TRS) approach [27,28] have been performed for ^{162}W . The total Routhian surfaces starting from the ground-state (quasiparticle vacuum) configuration are shown in Fig. 6. The minimum points in the energy surfaces are indicated by red (gray) dots. At zero rotational frequency, the minimum point indicated at $Y = -0.15$ (on the noncollective axis) is equivalent to the minimum at ($\beta_2 = 0.15, \gamma = 0^\circ$) on the prolate collective axis. A prolate ground-state shape is hence predicted with the quadrupole deformation parameter β_2 around 0.15. At a rotational frequency $\hbar\omega \approx 0.35$ MeV, the triaxial quadrupole deformation γ starts to increase and the β_2 deformation decreases. The TRS minimum then collapses into a noncollective structure. This might be associated with the alignment of a pair of $\nu f_{7/2}/h_{9/2}$ quasiparticles.

Analyzing the properties of the ground-state band of ^{162}W within a rotational collective framework provides further insights into the structure of the band. The experimental Routhians (energies in the rotating frame of the nucleus) are obtained by measuring the experimental level energies

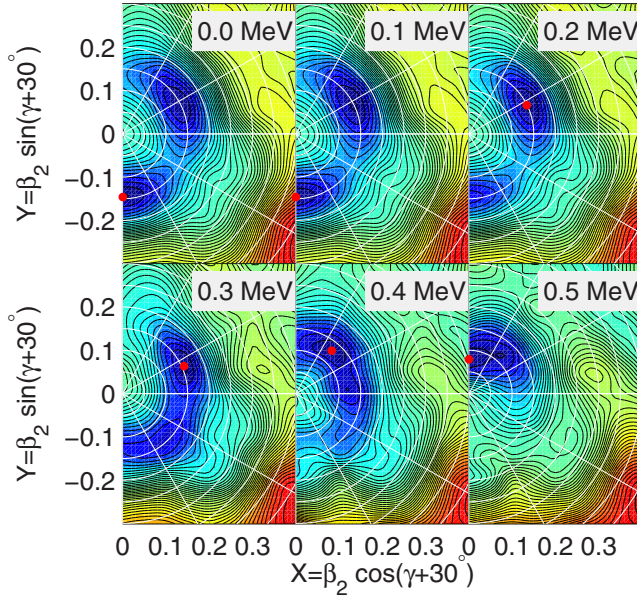


FIG. 6. (Color online) The TRS calculations for ^{162}W at $\hbar\omega = 0.0$ to 0.5 MeV. The energy difference between successive contour curves is 200 keV. Red (gray) dots indicate the positions of the minima in the surfaces.

in the laboratory frame with respect to a reference rotor. The degree of quasiparticle alignment can be observed in the plot of aligned angular momentum, i , versus rotational frequency, $\hbar\omega$, with respect to the same reference rotor. The experimental Routhians, e' , and alignments, i , are respectively expressed by

$$e'(\omega) = E'(\omega) - \omega I_x(\omega) - E_{\text{ref}}(\omega) \quad (1)$$

and

$$i(\omega) = I_x(\omega) - I_{\text{ref}}(\omega). \quad (2)$$

Here, $I_x(\omega)$ is the projection of total angular momentum along the rotational axis x and $E(I)$ is the energy at the intermediate value of the angular momentum I . The spin and energy of the reference configuration in the Harris description [29] are

$$I_{\text{ref}}(\omega) = \mathcal{J}_0\omega + \mathcal{J}_1\omega^3 \quad (3)$$

and

$$E_{\text{ref}}(\omega) = \frac{1}{8\mathcal{J}_0} - \frac{\omega^2}{2}\mathcal{J}_0 - \frac{\omega^4}{4}\mathcal{J}_1. \quad (4)$$

The extracted experimental Routhians and quasiparticle alignments versus rotational frequency are compared with the isotope ^{164}W [22] and isotope ^{160}Hf [26] in Fig. 7.

The ground-state band in ^{162}W exhibits a sharp increase in aligned angular momentum of $\Delta i \approx 6\hbar$ at $\hbar\omega \approx 0.30$ MeV. This alignment is slightly delayed and is significantly reduced in amplitude with respect to the observed band crossing in ^{164}W , which was assigned to be due to the first rotational alignment (AB) of a pair of $i_{13/2}$ neutrons [22]. However, at $N < 90$, the neutron Fermi level is significantly below the $i_{13/2}$ subshell and two-quasineutron alignments emanating from the mixed $f_{7/2}$ and $h_{9/2}$ subshells can compete with the

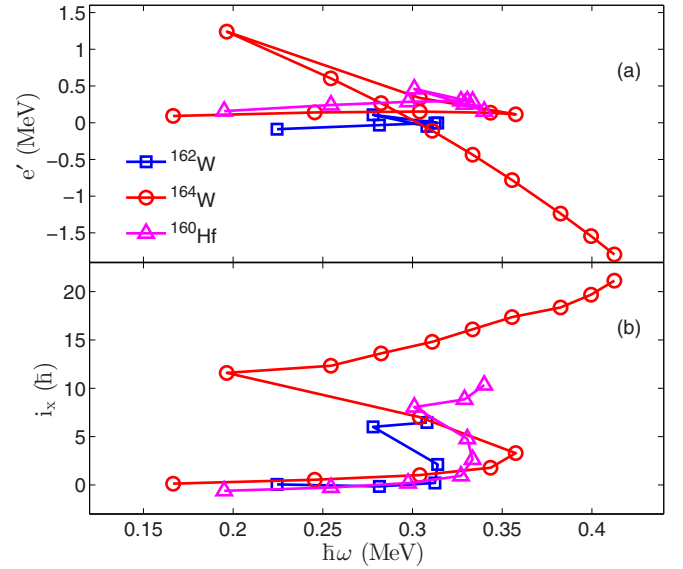


FIG. 7. (Color online) (a) Experimental Routhians and (b) aligned angular momenta for the ground-state bands in ^{162}W (present work), ^{164}W [22], and ^{160}Hf [26]. A rotational reference configuration has been subtracted using the Harris parameters $\mathcal{J}_0 = 1\hbar^2/\text{MeV}$ and $\mathcal{J}_1 = 196\hbar^4/\text{MeV}^3$, for ^{162}W , while those for ^{164}W and ^{160}Hf are taken from Refs. [22,26].

pure $i_{13/2}$ two-quasineutron alignment as discussed, e.g., by Dracoulis *et al.* [6]; see Fig. 8 (upper panel). The amount of aligned angular momentum might indicate that the S -band in ^{164}W is dominated by neutrons from the $f_{7/2}$ subshell. The isotone, ^{160}Hf , exhibits a further delayed band crossing at $\hbar\omega \approx 0.32$ MeV, with an intermediate value for the aligned angular momentum ($\Delta i_x \approx 8\hbar$), which seems to be followed by yet another band crossing at $\hbar\omega \approx 0.35$ MeV. A paired *quasiproton* band crossing originating from the $h_{11/2}$ subshell is predicted by our cranked shell model calculations [30,31], see Fig. 8 (lower panel), at similar rotational frequencies as that due to the $\nu(f_{7/2}/h_{9/2})^2$ alignment. Hence, it is possible that the alignments observed for ^{160}Hf are due to successive $\nu(f_{7/2}/h_{9/2})^2/\pi(h_{11/2})^2$ band crossings and that the difference compared with ^{162}W is due to a difference in shape and position of the proton Fermi level. However, note that Murzel *et al.* [26] assigned the first band crossing in ^{160}Hf to a $\nu(i_{13/2})^2$ AB quasiparticle alignment and discussed the reduced aligned angular momentum compared with the CSM predictions in terms of γ softness of the nuclear potential.

The nuclear structure effect on the α decay is carried by the so-called α -formation probability on the nuclear surface, which can be extracted from the experimental α -partial half-life and decay value, Q , as in Refs. [33–35]. As discussed in the above references, in most cases the experimental α -formation probabilities show a rather smooth behavior when going from a nucleus to its neighboring nuclei, which is related to the fact that the α clustering is dominated by the slowly varying nuclear pairing correlations. As a result, the abrupt change in the systematics of α -formation probability would indicate a transition in the underlying nuclear structure. In Fig. 9, we plotted the experimental α formation probabilities thus

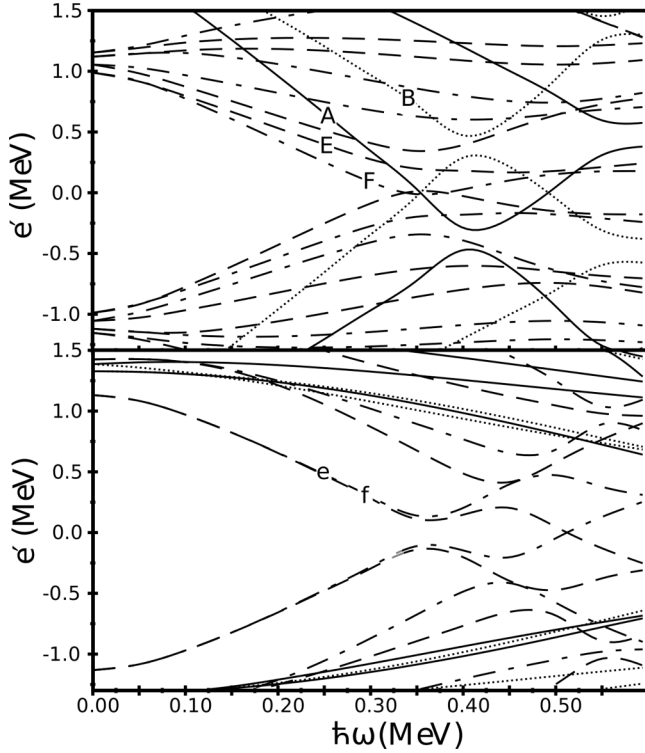


FIG. 8. Cranked Routhians using the universal Woods-Saxon potential for quasineutrons (upper panel) and quasiprotons (the lower panel) in ^{162}W with the deformation parameters $\beta_2 = 0.146$, $\beta_4 = 0.010$, and $\gamma = 0^\circ$ taken from TRS predictions. Different lines represent different parities and signatures (π, α): solid denotes (+, +1/2), dotted denotes (+, -1/2), dot-dashed denotes (-, +1/2), and dashed denotes (-, -1/2). Quasiparticle alignments due to a pair of $h_{11/2}$ protons are predicted at $\hbar\omega \approx 0.36$ MeV while $f_{7/2}/h_{9/2}$ and $i_{13/2}$ neutrons are predicted to align at $\hbar\omega \approx 0.36$ and $\hbar\omega \approx 0.41$ MeV, respectively. The shell model labelings for quasiparticles in ^{162}W are marked as below: A, $\nu i_{13/2}$ with positive signature; B, $\nu i_{13/2}$ with negative signature; E, $\nu f_{7/2}/h_{9/2}$ with negative signature; F, $\nu f_{7/2}/h_{9/2}$ with positive signature; e, $\pi h_{11/2}$ with negative signature; and f, $\pi h_{11/2}$ with positive signature.

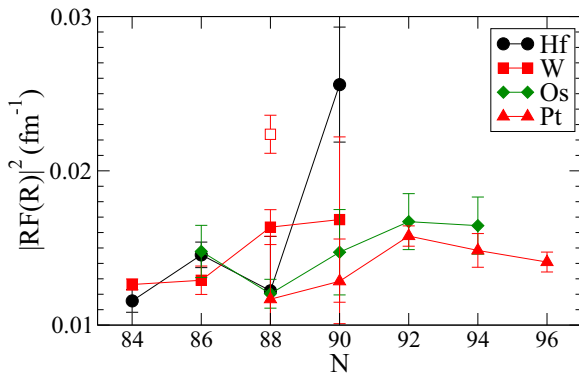


FIG. 9. (Color online) α -formation probabilities $|\text{RF}(\text{R})|^2$ calculated from experimental α -decay partial half-lives as a function of the neutron number, N , for the α decays of even-even Hf, W, Os, and Pt isotopes. The experimental data represented by solid symbols are from NNDC [32]. Our new data for ^{162}W is shown as the open symbol.

calculated for the α decays of even-even W isotopes and neighboring Hf, Os, and Pt isotopes as a function of neutron number, N . The new result on ^{162}W is included by taking the α -decay branching ratio as $b = 44(2)\%$ [18]. As can be seen from Fig. 9, the α -formation probability extracted from our new half-life (open symbol) is significantly larger than that deduced from the adopted values and those of most neighboring nuclei, making it one of the most favored α emitters in this region. However, it should be noted that there are variations in reported α -decay branching ratios and half-lives in the literature that deserve further attention. For example, the α -formation probability of ^{164}W is $|\text{RF}(\text{R})|^2 = 0.017(5) \text{ fm}^{-1}$ taking the branching ratio and half-life from Ref. [32], while the corresponding value is $0.023(5)$ if we take the information from Ref. [18].

IV. SUMMARY

Excited states in the neutron-deficient nuclide ^{162}W have been identified using the highly selective RDT technique. A ground-state rotational-like band structure was established up to $I^\pi = (12^+)$, confirming the previous results reported by Dracoulis *et al.* [6]. Quasiparticle alignment effects are discussed based on cranked shell model calculations and the observed paired band crossing is suggested to be associated with the alignment of a pair of $\nu f_{7/2}/h_{9/2}$ quasiparticles. Total Routhian surface (TRS) calculations predict an axially symmetric ground-state shape with a γ -soft minimum at $\beta_2 \approx 0.15$. New measurements of the ^{162}W ground-state α -decay energy and half-life were also performed. The observed α -decay energy agrees with previous measurements. The half-life of ^{162}W was determined to be $t_{1/2} = 990(30)$ ms. This value deviates significantly from the currently adopted value of $t_{1/2} = 1360(70)$ ms. In addition, the α -decay energy and half-life of ^{166}Os were measured and found to agree with the adopted values. The α -formation probability for ^{162}W is also extracted from the measured half-life and compared systematically with those of neighboring nuclei. A large enhancement compared with typical values is noted.

ACKNOWLEDGMENTS

The authors thank the staff at the Accelerator Laboratory of the University of Jyväskylä for their excellent technical support. Support for this work was given by the Swedish Research Council (Contract No. 2010-3694), the Academy of Finland under the Finnish Centre of Excellence Programme 2012–2017, the UK Science and Technology Facilities Council, and the European Union Seventh Framework Program Integrating Activities–Transnational Access Project No. 262010 (ENSAR). H. J. Li is supported in part by the China Scholarship Council under Grant No. 201306210205. T.G acknowledges the support from the Academy of Finland (Contract No. 131665). Additionally, we thank the EUROBALL owners committee (γ -pool network) and the UK/France (EPSRC/IN2P3) detector loan pool for providing the EUROGAM detectors of JUROGAM II.

- [1] K. Heyde and J. L. Wood, *Rev. Mod. Phys.* **83**, 1467 (2011).
- [2] K. Heyde and J. L. Wood, *Rev. Mod. Phys.* **83**, 1655 (2011).
- [3] K.-H. Schmidt, R. S. Simon, J.-G. Keller, F. P. Hessberger, G. Münzenberg, B. Quint, H.-G. Clerc, W. Schwab, U. Gollerthan, and C.-C. Sahm, *Phys. Lett. B* **168**, 39 (1986).
- [4] R. S. Simon, K.-H. Schmidt, F. P. Hessberger, S. Hlavac, M. Honusek, G. Münzenberg, H.-G. Clerc, U. Gollerthan, and W. Schwab, *Z. Phys. A* **325**, 197 (1986).
- [5] E. S. Paul *et al.*, *Phys. Rev. C* **51**, 78 (1995).
- [6] G. D. Dracoulis *et al.*, Proc. Int. Conf. Nuclear Structure at High Angular Momentum, Ottawa **2**, 94 (1992).
- [7] M. J. Taylor *et al.*, *Nucl. Instrum. Methods Phys. Res. A* **707**, 143 (2013).
- [8] C. W. Beausang *et al.*, *Nucl. Instrum. Methods Phys. Res. A* **313**, 37 (1992).
- [9] C. R. Alvarez, *Nucl. Phys. News* **3**, 10 (1993).
- [10] G. Duchêne, F. A. Beck, P. J. Twin, G. de France, D. Curien, L. Han, C. W. Beausang, M. A. Bentley, P. J. Nolan, and J. Simpson, *Nucl. Instrum. Methods Phys. Res. A* **432**, 90 (1999).
- [11] P. Ruotsalainen *et al.*, *Phys. Rev. C* **88**, 024320 (2013).
- [12] M. Leino *et al.*, *Nucl. Instr. Meth.* **99**, 653 (1995).
- [13] M. Leino, *Nucl. Instr. Meth. B* **126**, 320 (1997).
- [14] R. D. Page *et al.*, *Nucl. Instrum. Methods Phys. Res., Sect. B* **204**, 634 (2003).
- [15] I. H. Lazarus *et al.*, *IEEE Trans. Nucl. Sci.* **48**, 567 (2001).
- [16] P. Rahkila, *Nucl. Instr. Meth. A* **595**, 637 (2008).
- [17] D. C. Radford, *Nucl. Instrum. Meth. A* **361**, 297 (1995).
- [18] R. D. Page *et al.*, *Phys. Rev. C* **53**, 660 (1996).
- [19] C. W. Reich, *Nucl. Data Sheets* **108**, 1807 (2007).
- [20] S. Hofmann *et al.*, *Z. Phys. A* **333**, 107 (1989).
- [21] A. Keenan *et al.*, *Phys. Rev. C* **63**, 064309 (2001).
- [22] J. Simpson, M. A. Riley, A. Alderson, M. A. Bentley, A. M. Bruce, D. M. Cullen, P. Fallon, F. Hanna, and L. Walker, *J. Phys. G: Nucl. Part. Phys.* **17**, 511 (1991).
- [23] J. Simpson, F. Hanna, M. A. Riley, A. Alderson, M. A. Bentley, A. M. Bruce, D. M. Cullen, P. Fallon, and L. Walker, *J. Phys. G: Nucl. Part. Phys.* **18**, 1207 (1992).
- [24] K. Theine *et al.*, *Nucl. Phys. A* **548**, 71 (1992).
- [25] D. T. Joss *et al.*, *Phys. Rev. C* **70**, 017302 (2004).
- [26] M. Murzel *et al.*, *Nucl. Phys. A* **516**, 189 (1990).
- [27] W. Nazarewicz *et al.*, *Nucl. Phys. A* **503**, 285 (1989).
- [28] W. Satula and R. Wyss, *Phys. Scr.* **T56**, 159 (1995).
- [29] S. M. Harris, *Phys. Rev.* **138**, B509 (1965).
- [30] W. Nazarewicz, J. Dudek, R. Bengtsson, T. Bengtsson, and I. Ragnarsson, *Nucl. Phys. A* **435**, 397 (1985).
- [31] S. Ćwiok, J. Dudek, W. Nazarewicz, J. Skalski, and T. Werner, *Comput. Phys. Commun.* **46**, 379 (1987).
- [32] <http://www.nndc.bnl.gov/>
- [33] C. Qi, F. R. Xu, R. Liotta, R. Wyss, M. Zhang, C. Asawatangtrakuldee, and D. Hu, *Phys. Rev. C* **80**, 044326 (2009).
- [34] C. Qi, A. N. Andreyev, M. Huyse, R. J. Liotta, P. Van Duppen, and R. A. Wyss, *Phys. Rev. C* **81**, 064319 (2010).
- [35] A. N. Andreyev *et al.*, *Phys. Rev. Lett.* **110**, 242502 (2013).